MedChemComm

CONCISE ARTICLE

Rhodanine carboxylic acids as novel inhibitors of histone acetyltransferases†‡

Silviya D. Furdas,[a] **Suhaib Shekfeh,**[b] **Srinivasaraghavan Kannan,**[b] **Wolfgang Sippl**[b] **and Manfred Jung*[a]**

Histone acetyltransferases (HATs) are promising epigenetic drug targets and are involved in the pathogenesis of a wide range of diseases. We carried out a virtual screening based on inhibitors of serotonin *N*-acetyltransferase and identified novel inhibitors of the HAT PCAF with a 2-thioxo-4-thiazolidinone (rhodanine) scaffold attached to a long chain carboxylic acid. Their binding mode was studied by means of docking and molecular dynamics simulations. Structure–activity studies were performed by organic synthesis and *in vitro* testing in an antibody based biochemical assay showing similar inhibition on the HATs PCAF, Gcn5, CBP and p300 *in vitro*. In contrast, a pyridoisothiazolone reference inhibitor is more potent on CBP and to some extent on PCAF but less potent on Gcn5. Structural elements were identified that provide the basis for further optimization of the new inhibitors.

Introduction

Reversible lysine acetylation in proteins is an important mechanism for epigenetic gene regulation and for the regulation of the activity of non-histone proteins. The transfer of the acetyl residue from the cosubstrate acetyl-CoA is catalyzed by histone acetyltransferases (HATs) and leads in the case of histone substrates to an open form of eukaryotic chromatin (euchromatin). Deacetylation of histone lysine residues by histone deacetylases (HDACs) will globally impede transcription.[1] Lysine acetylation is involved in many cellular events like differentiation, gene expression, vascular remodeling, neuronal plasticity, inflammation, and metabolism and points to many possible therapeutic applications.[2–7] Especially, links to the pathogenesis of cancer are well described.[8–10] Among the hundreds of non-histone substrates[11,12] for HATs some important examples are p53,[13] α-tubulin,[14,15] c-myc,[16,17] c-fos, c-jun,[18] cohesin,[19] NF-κB,[20] interleukins,[21] androgen receptor,[22] HIV-1 Tat protein,[23] MyoD,[24] FoxO,[25] and E2F1.[26] Hence, HATs have also been termed as lysine acetyltransferases (*KATs*) in a more general way.[27]

There is a wide range of HAT inhibitors available[28–30] but only a few of them are drug-like. Examples for different classes of HAT inhibitors are pyridoisothiazolones like **1**,[31] analogues of anacardic acid like **2**[32] or **3**,[33] and pyrazolone benzoic acids like C646, **4**[34] (Fig. 1).

In this study, we set out to find novel scaffolds for new HAT inhibitors using virtual screening on the structurally related serotonin *N*-acetyltransferase, also termed arylalkylamine *N*-acetyltransferase (AANAT), and succeeded in identifying rhodanine carboxylic acids as novel lead structures.

Virtual screening

In order to identify new inhibitors of HATs, we applied a strategy that combines computational screening methods with robust biochemical assays that has been successfully applied to several targets recently.[35–37] Virtual database filtering was used to conduct a virtual screening. As a starting point, we used rhodanine–indolinone derivatives (Fig. 2), which have been recently identified as inhibitors of the homologue serotonin *N*-acetyltransferase AANAT which also belongs to the GNAT family of acetyltransferases.[38]

Subsequently, the initial hits were docked into the active site of PCAF. In the PCAF crystal structure CoA is bound in
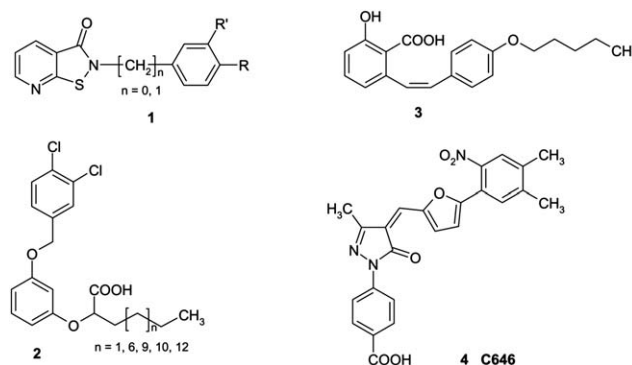
[a]Institute of Pharmaceutical Sciences, Albert-Ludwigs-Unversity of Freiburg, Albertstr. 25, 79104 Freiburg, Germany. E-mail: manfred.jung@pharmazie.uni-freiburg.de; Fax: +49-761-203-6321; Tel: +49-761-203-4896

[b]Department of Pharmaceutical Chemistry, Martin-Luther University of Halle-Wittenberg, Germany

† Electronic supplementary information (ESI) available: Computational methods, molecular dynamics results, experimental procedures (enzyme preparation, biological testing, and synthesis), and spectroscopic characterization of all new compounds. See DOI: 10.1039/c2md00211f
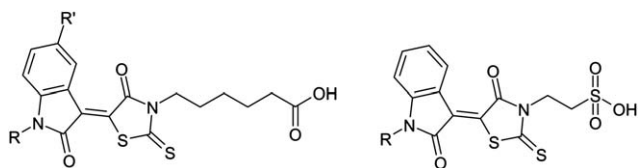‡ This article is part of a *MedChemComm* web themed issue on epigenetics.

Fig. 1 HAT inhibitors from the literature.

Fig. 2 Bisubstrate AANAT inhibitors from the literature.[38]

a conformation where it forms an extensive set of protein inter-
actions that are mediated predominantly by the pantetheine arm
and the pyrophosphate group[39] with motif A–D and motif B of
the enzyme (Fig. 3).

GNAT conserved residues in PCAF motifs A and B interact
extensively with CoA. Residues 580 and 582–587 in the β4 loop
α3 region of motif A make direct and water-mediated hydrogen
bonds with the pyrophosphate group, similar to the binding
mode of CoA in the serotonin *N*-acetyltransferase AANAT.[40]
The aliphatic side chain of Gln581 and a Cys-Ala-Val sequence
(residues 574–576) at the top of the β4-strand make van der
Waals contacts with the aliphatic part of the pantetheine arm[39]
(Fig. 3 and 4).

We used a synergistic approach that combines the benefits of
structure-based virtual screening and experimental testing which
validated a PCAF inhibition assay to subsequently screen only
a limited number of the top-ranking compounds. We carried out
a multi-step virtual screening experiment starting with a simi-
larity based screening followed by docking. MACCS fingerprints
derived from the rhodanine–indolinone AANAT inhibitors were
used for a search query in 21 commercial databases. A total of
6423 compounds was identified from the *in silico* screening and
subsequently docked into the PCAF substrate binding site to test
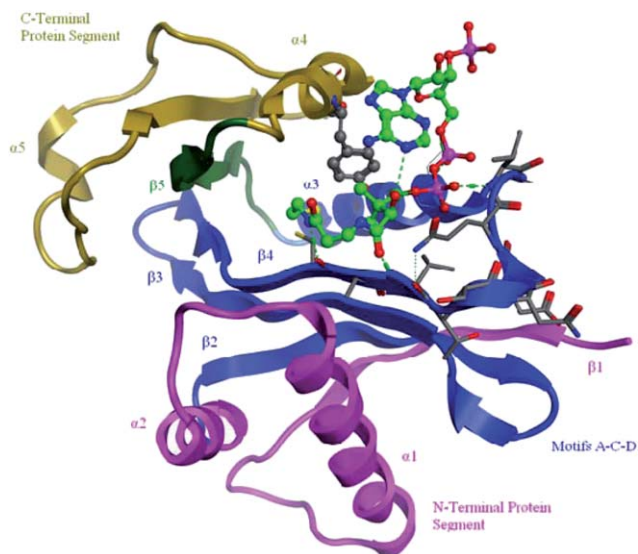whether they are able to bind at the CoA binding site. The crystal

Fig. 3 Structure of the PCAF–CoA complex representing the general
secondary structure of GNAT family acetyltransferases and the location
of the acetylCoA binding site. The four domains of the protein are color-
coded. Motifs A–D and motif B (based on structural conservation) are
colored blue and green, respectively. The *N*- and *C*-terminal protein
segments flanking the core are colored magenta and gold, respectively.
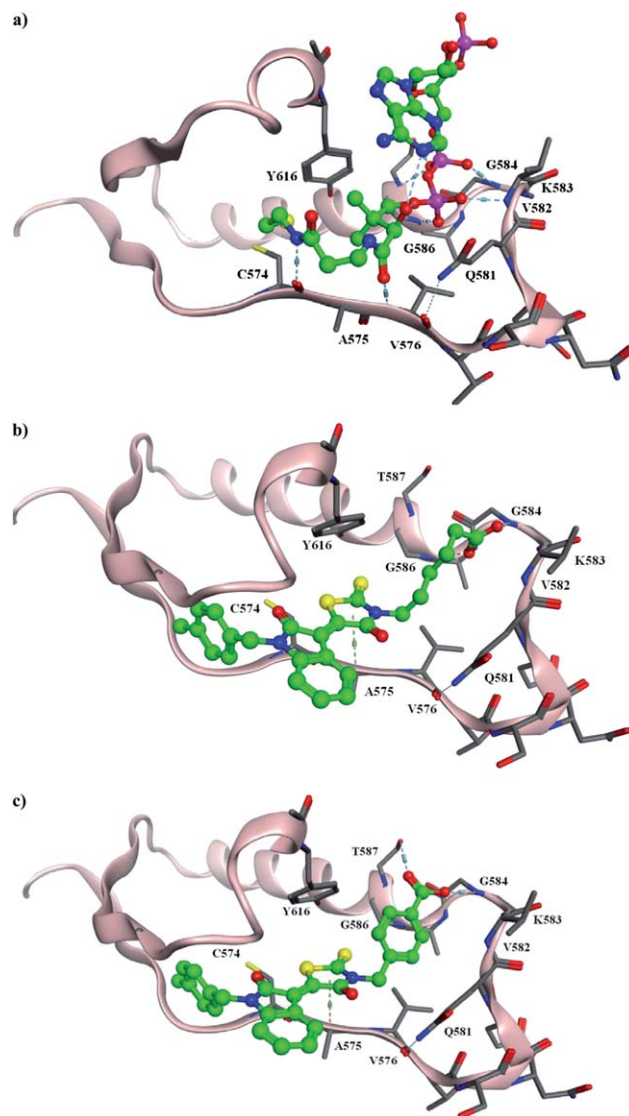CoA is colored light green. Y616 is shown in capped sticks colored grey.

Fig. 4 (a) Interaction of CoA in the PCAF crystal structure. (b) Docking
pose calculated for compound **12e**. (c) Docking pose calculated for
compound **14**. Ligands are shown in green color, hydrogen bonds are
displayed as dashed lines. Only relevant amino acids are displayed.

structure of PCAF complexed with the cofactor acetyl-CoA (pdb
code: 1CM0) was used for docking studies. Goldscore and
Chemscore were considered as scoring functions. A visual
inspection was carried out for the 100 top ranked solutions and
11 compounds were further considered for biological testing
(Fig. 5).

The predicted binding mode for the rhodanine–indolinone–
carboxylate analogs suggests that the inhibitor's acidic group,
aliphatic linker as well the rhodanine ring interact with the
cofactor binding pocket whereas the rest of the inhibitor interacts
with the substrate binding pocket (Fig. 4). Molecular interaction
fields further support the predicted binding mode. They indicated
the strongest affinity for a carboxylic group in the region around
the residues Val582 and Gly586 where the pyrophosphate part of
CoA is interacting. On the other hand, the highest affinity for
a hydrophobic probe exists in the neighborhood of the reaction
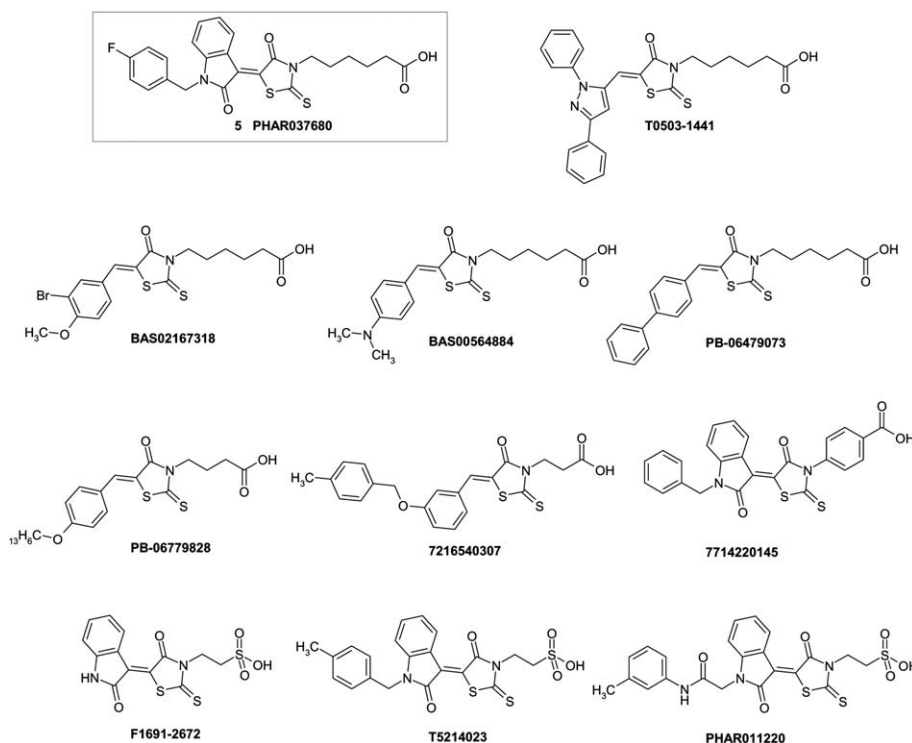center where the cofactor's sulfur is located (Fig. S1 in the ESI†).

Fig. 5 Selected compounds from the virtual screening with thiazolidinone scaffold.

Initial *in vitro* testing

For the determination of *in vitro* inhibition we used a heterogeneous assay with antibody mediated quantitation of acetylation and time-resolved fluorescence as the final readout. As the enzyme source we used the catalytic domain (aa 493–658) of human recombinant PCAF (*KAT2B*) expressed in *E. coli*. Among the virtual screening hits, 11 rhodanines could be ordered from commercial sources. The chemical structures of the carboxylic acid derivatives are presented in Fig. 4. In general, compounds with a carboxylic moiety exhibited stronger PCAF inhibitory properties compared to rhodanine–indolinone derivatives with a sulfonic acid function (Table 1). Compounds without the indolinone moiety were inactive. Furthermore, due to the suggestion that the COOH group is essential for HAT inhibition, four commercially available 5-arylidene-2-thioxo-4-thiazolidinone substituted methyl esters with different alkyl chain lengths (Fig. 6) have been tested for PCAF inhibition *in vitro*. As expected, at the selected initial concentration for screening of 50 μM all those esters inhibited PCAF by less than 25%. This supports the assumption that a free carboxylic acid is required for inhibition. The most promising compound was **5** (PHAR037680), which is related to AANAT inhibitors from the literature.[38] It consists of an *N*-benzylated indolinone that is condensed with a rhodanine carboxylic acid. It displayed an IC$_{50}$ value against PCAF of 98 μM and was selected for structure–activity studies.

Synthesis and PCAF inhibition of analogues

We identified two structural elements that could be modified in the first round of variation: (a) variation or replacement of the *N*-benzyl-moiety and (b) variation of the aliphatic spacer length resp. rigidification within a ring structure (Fig. 7). As the first methyl esters that were tested have a different substitution pattern than our lead inhibitor, a structurally corresponding methyl ester was tested in order to further underline the hypothesis that a free carboxylic acid moiety is crucial for HAT inhibition *in vitro*.

Towards that end, we set up a convergent route of synthesis centered around the condensation of the *N*-alkylated

Table 1 Inhibition of PCAF histone acetyltransferase activity for histone substrate H3 (amino acid residues 1–21); IC$_{50}$ value [μM] ± standard error [μM] or enzyme inhibition [%] at the specified concentration for purchased compounds (Fig. 5 and 6)[a]

	Compound (Supplier)	HAT inhibition: PCAF, H3$_{aa1-21}$
Carboxylic acids	**PHAR037680** (PHARMEKS) **5**	97.7 ± 10.4 μM
	T0505-1441 (Enamine)	12% @ 50 μM
	BAS02167318 (Asinex)	8% @ 50 μM
	BAS0056484 (Asinex)	n.i. @ 50 μM
	PB-06479073 (UkrOrgSynth)	n.i. @ 50 μM
	PB-06779828 (UkrOrgSynth)	8% @ 50 μM
	7216540307 (Otava)	5% @ 50 μM
	7714220145 (Otava)	14% @ 50 μM
Sulfonic acids	**F1691-2672** (Life Chemicals)	n.i. @ 50 μM
	T5214023 (Enamine)	n.i. @ 50 μM
	PHAR011220 (PHARMEKS)	6% @ 50 μM
Methyl esters	**3130–0992** (ChemDiv)	8% @ 50 μM
	3643–3094 (ChemDiv)	9% @ 50 μM
	3643–3114 (ChemDiv)	21% @ 50 μM
	3643–3103 (ChemDiv)	24% @ 50 μM

[a] n.i.: no enzyme inhibition (<5%) at the specified assay concentration.

indolinedione[41] with the CH-acidic rhodanine that is already *N*-alkylated with the carboxylic acid spacer (Scheme 1). The latter was synthesized from carbon disulfide, chloroacetic acid, and an ω-amino acid according to standard procedures.[42] For incorporation of 4-aminomethylbenzoic acid and tranexamic acid we used an alternative route to the rhodanine, employing bis(carboxymethyl)trithiocarbonate as the sulfur donating reagent.[43] The final step constitutes a Knoevenagel-type condensation of the active methylene group (rhodanine moiety) with the keto group of the α-ketoamide (indolinone moiety).[44]

The obtained compounds with a core scaffold as presented in Fig. 8 were then tested in the same *in vitro* assay as the initial screening hit **5** (Fig. 4). The results are displayed in Table 2. The reference inhibitor **1a** (see Fig. 1, n = 1, R =Cl, R′ = H) was used as a structurally unrelated control.[31]

The results showed that a substituted benzyl substituent on the indolinone moiety is necessary for inhibition below 100 μM (Table 1). The *N*-unsubstituted compound **12a** as well as the methyl **12b**, ethyl **12c**, and even the benzyl analogue **12d** did not show significant inhibition. Among the 4-substituted benzyl congeners, the compounds with electropositive substitution

(methyl **12e** and methoxy **12f**) were more potent than the nitro derivative **12g**. The binding mode of the methyl substituted analog **12e** shows a positioning of the thioester and thiocarbonyl of rhodanine ring beside the central Cys574 while the carboxylate makes hydrogen bonds with residues Val582, Gly584, and Gly586. The benzyl group, which is attached to the indolinone ring, is deeply positioned inside the substrate binding pocket (Fig. 4). Shortening the alkyl spacer by only one methylene group in **13** led to a strong decrease in activity but rigidification within a 1,4-phenylene **14** or a *trans*-cyclohexylene **15** spacer was possible and in the case of the latter led to an increase of inhibitory activity. The cyclic linkers keep approximately the same length as the pentyl group between the rhodanine and the carboxylate group. Docking studies showed that this length of the linker is necessary to maintain the binding mode, where the carboxylic group is interacting with Val582, the rhodanine's sulfur is positioned beside the Cys574 and the benzyl group on the indolinone is positioned deeply inside the substrate binding pocket (Fig. 4). Docking solutions suggest positioning of that substituted benzyl group close to residue Tyr640 which is deeply buried in the binding site. The molecular interaction field calculated with a hydrophobic C3 probe shows a favourable field in that region (Fig. S1, ESI†). The corresponding methyl ester **16** of compound **12e** was also inactive. The most potent inhibitors were also tested on the commercially available HATs Gcn5, CBP, and p300 and were shown to be unselective on all the subtypes with IC$_{50}$ values at the micromolar level (Table 3). Interestingly, the reference inhibitor shows a tenfold selectivity for CBP over PCAF and a greatly reduced inhibition of Gcn5. Due to thiols in the buffer of the commercially available p300, we could not test **1a** on this subtype.
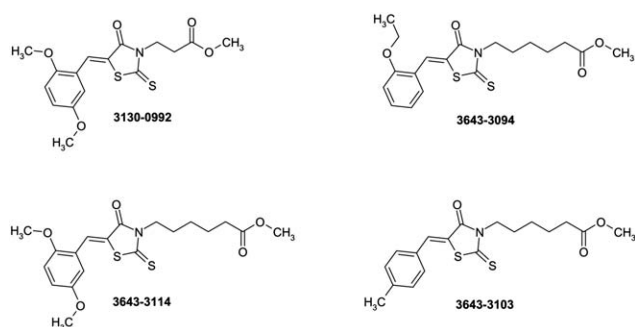

Fig. 6 Selected methyl esters with thiazolidinone scaffold from the virtual screening.

MD simulations

To further validate the predicted binding mode and to assess the stability of docked complex MD simulations were employed. The
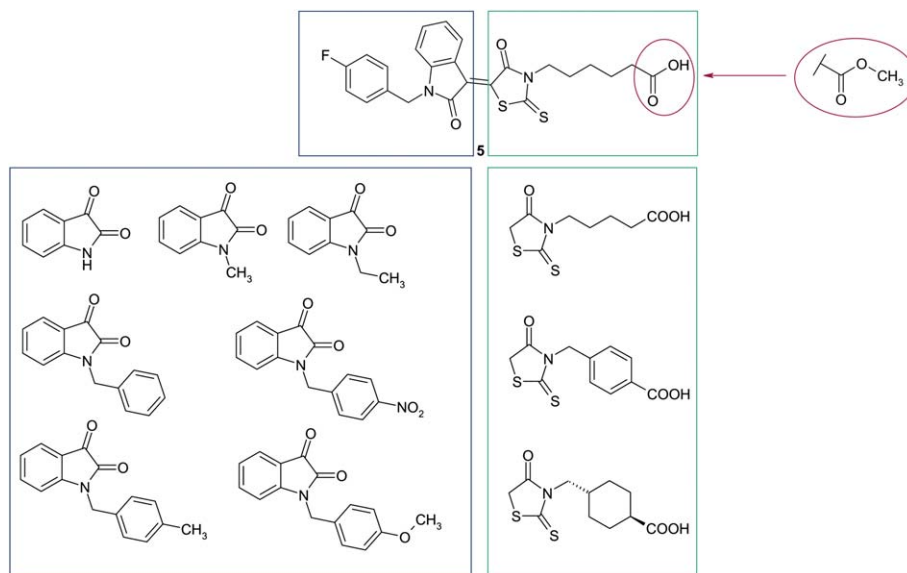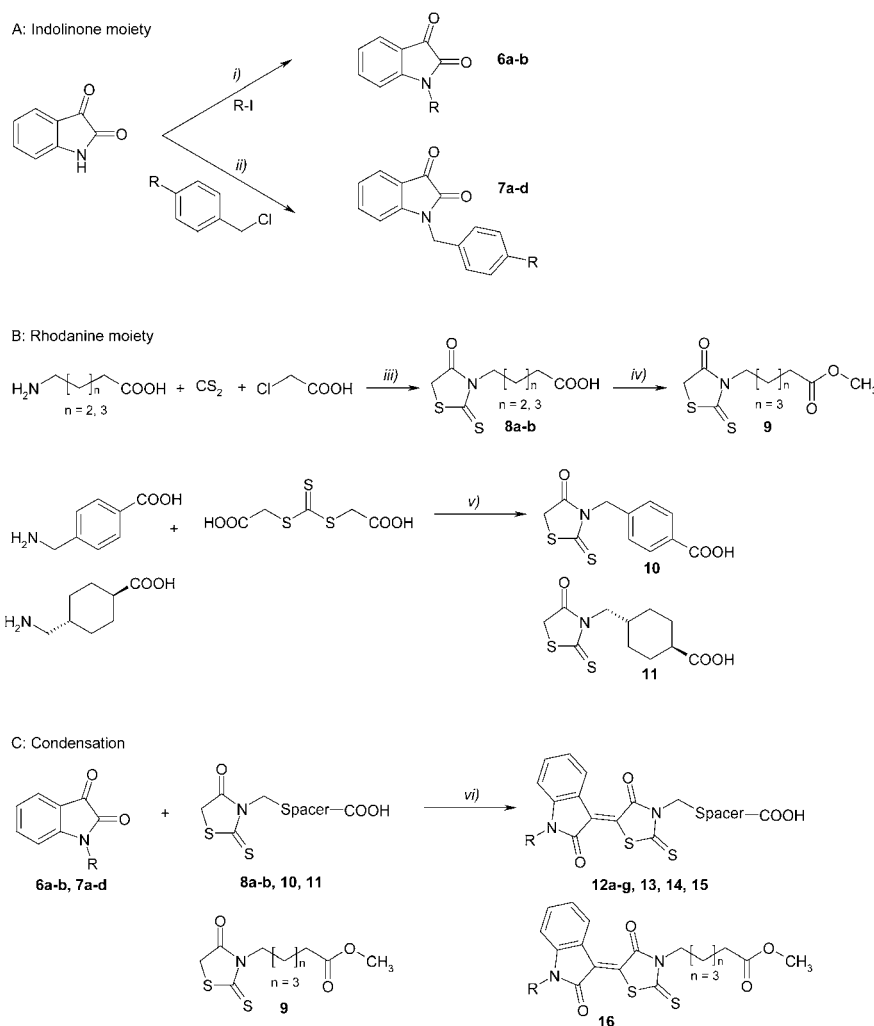

Fig. 7 Variation of the lead structure PHAR037680 **5** concerning the substitution pattern of the rhodanine–indolinone core.

308 | *Med. Chem. Commun.*, 2012, **3**, 305–311

This journal is © The Royal Society of Chemistry 2012

Scheme 1 Synthesis routes: (A): *Indolinone moiety* (i) K_2CO_3, CH_3CN, rt, ~30 h; (ii) K_2CO_3, KI, CH_3CN, rt, ~30 h; (B): *rhodanine moiety* (iii) KOH, conc. H_2SO_4, H_2O, rt, overnight; (iv) $SOCl_2$, CH_3OH, −20 °C → rt, overnight; (v) Na_2CO_3, dil. H_2SO_4, H_2O, reflux, overnight; (C): *condensation* (vi) C_2H_5OH, reflux, ~20 h; (rt: room temperature).
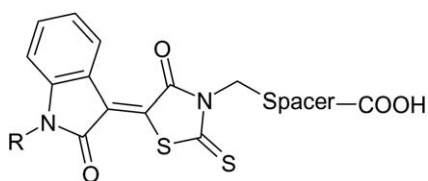

Fig. 8 Rhodanine–indolinone scaffold for synthesized compounds **12a–g** and **13–15**.

PCAF–inhibitor complexes derived from the docking study were used as starting complexes for molecular dynamics (MD) simulations using the AMBER program. These simulations showed that the generated complexes are stable during the 10 ns MD simulation. As an example, the root mean square deviation (RMSD) of sampled conformations of compound **12e** calculated against the initial docked conformation shows that complexes reach the stable conformation at around 2 ns and this stability is maintained during the rest of simulation. The inhibitor interactions observed in the starting structures (obtained by GOLD) were generally maintained during the MD simulations (RMSD plot of compound **12e** is shown as example in Fig. S2 in the ESI†).
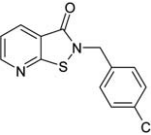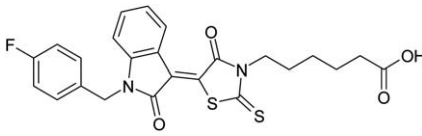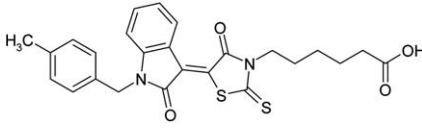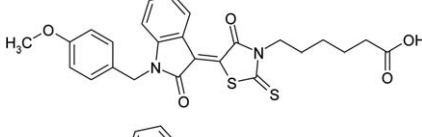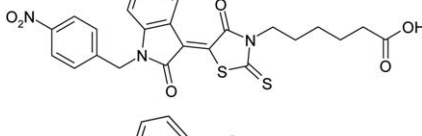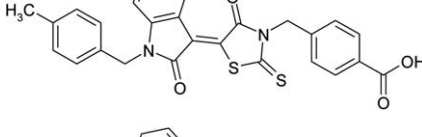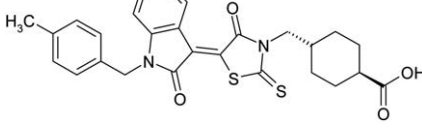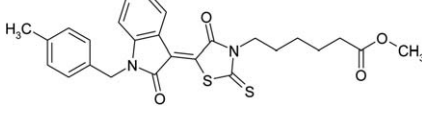
Conclusion

We have successfully performed a virtual screening campaign towards new lead inhibitors for HATs. Rhodanine carboxylic acids are new unselective HAT inhibitors with activity in the two-digit micromolar range. Initial structure–activity relationships have better determined the pharmacophore, and the beneficial effect of certain structural elements (4-methoxybenzyl group, *trans*-cyclohexylene spacer) points out directions for further optimization. The new inhibitors are broadband HAT inhibitors while a pyridoisothiazolone reference inhibitor was shown to possess increased activity on CBP and to some extent on PCAF but is less potent on Gcn5.

Table 2 Inhibition of PCAF histone acetyltransferase activity for histone substrate H3 (amino acid residues 1–21); IC$_{50}$ value [μM] ± standard error [μM] or enzyme inhibition [%] at the specified concentration for synthesized compounds according to the scaffold in Fig. 8

Cpd.	Spacer	R	PCAF, H3$_{aa1-21}$
12a	C$_4$H$_8$ *butylene*	H	9% @ 50 μM
12b	C$_4$H$_8$ *butylene*	CH$_3$ *methyl*	5% @ 50 μM
12c	C$_4$H$_8$ *butylene*	C$_2$H$_5$ *ethyl*	6% @ 50 μM
12d	C$_4$H$_8$ *butylene*	(C$_6$H$_5$)CH$_2$ *benzyl*	13% @ 50 μM
12e	C$_4$H$_8$ *butylene*	4-CH$_3$(C$_6$H$_5$)CH$_2$ *4-methylbenzyl*	67.2 ± 2.3 μM
12f	C$_4$H$_8$ *butylene*	4-OCH$_3$(C$_6$H$_5$)CH$_2$ *4-methoxybenzyl*	28.8 ± 2.1 μM
12g	C$_4$H$_8$ *butylene*	4-NO$_2$(C$_6$H$_5$)CH$_2$ *4-nitrobenzyl*	78.2 ± 3.6 μM
13	C$_3$H$_6$ *propylene*	4-CH$_3$(C$_6$H$_5$)CH$_2$ *4-methylbenzyl*	8% @ 50 μM
14	C$_6$H$_4$ *phenylene*	4-CH$_3$(C$_6$H$_5$)CH$_2$ *4-methylbenzyl*	63.7 ± 1.6 μM
15	C$_6$H$_{10}$ *trans-cyclohexylene*	4-CH$_3$(C$_6$H$_5$)CH$_2$ *4-methylbenzyl*	41.8 ± 4.2 μM

Table 3 Inhibition of selected members of the HAT histone acetyltransferase family for histone substrate H3 (amino acid residues 1–21); IC$_{50}$ value [μM] ± standard error [μM] or enzyme inhibition [%] at the specified concentration for control inhibitor **1a**, lead structure **5**, and synthesized compounds **12e–g** and **14–16**[ab]

Cpd.	Structure	Gcn5 (KAT2A$_{aa362-837}$)	PCAF (KAT2B$_{aa493-658}$)	CBP (KAT3A$_{aa1319-1710}$)	p300 (KAT3B$_{aa965-1810}$)
1a		89.9 ± 2.7 μM	17.5 ± 1.3 μM (lit[31])	1.95 ± 0.4 μM	n.t.
5		209.6 ± 3.2 μM	97.7 ± 10.4 μM	115.7 ± 4.0 μM	244.1 ± 30.1 μM
12e		47.0 ± 1.8 μM	67.2 ± 2.3 μM	41.0 ± 1.4 μM	81.0 ± 6.7 μM
12f		54.7 ± 6.2 μM	28.8 ± 2.1 μM	40.9 ± 1.6 μM	61.9 ± 4.4 μM
12g		69.6 ± 1.8 μM	78.2 ± 3.6 μM	28.4 ± 7.7 μM	151.9 ± 6.4 μM
14		63.5 ± 4.2 μM	63.7 ± 1.6 μM	35.9 ± 3.4 μM	95.3 ± 10.7 μM
15		46.4 ± 2.7 μM	41.8 ± 4.2 μM	38.5 ± 4.9 μM	23% @ 100 μM
16		6% @ 50 μM	8% @ 50 μM	25% @ 50 μM	n.i. @ 50 μM

[a] n.t.: not tested (due to thiols in the enzyme buffer which inactivate **1a**). [b] n.i.: no enzyme inhibition (<5%) at the specified assay concentration.

Acknowledgements

References

1 B. D. Strahl and C. D. Allis, *Nature*, 2000, **403**, 41–45.
2 P. J. Barnes, *Proc. Am. Thorac. Soc.*, 2009, **6**, 693–696.
3 A. P. Feinberg, *Nature*, 2007, **447**, 433–440.
4 A. Johnsson, M. Durand-Dubief, Y. Xue-Franzen, M. Ronnerblad, K. Ekwall and A. Wright, *EMBO Rep.*, 2009, **10**, 1009–1014.
5 B. Keenen and I. L. de la Serna, *J. Cell. Physiol.*, 2009, **219**, 1–7.
6 D. Pons and J. W. Jukema, *Neth. Heart J.*, 2008, **16**, 30–32.
7 B. R. Selvi, J. C. Cassel, T. K. Kundu and A. L. Boutillier, *Biochim. Biophys. Acta, Gen. Subj.*, 2009, **1799**, 840–853.
8 L. Ellis, P. W. Atadja and R. W. Johnstone, *Mol. Cancer Ther.*, 2009, **8**, 1409–1420.
9 M. Esteller, *Br. J. Cancer*, 2007, **96**(Suppl), R26–R30.
10 M. Esteller, *N. Engl. J. Med.*, 2008, **358**, 1148–1159.
11 C. Choudhary, C. Kumar, F. Gnad, M. L. Nielsen, M. Rehman, T. C. Walther, J. V. Olsen and M. Mann, *Science*, 2009, **325**, 834–840.
12 K. L. Norris, J. Y. Lee and T. P. Yao, *Sci. Signaling*, 2009, **2**, pe76.
13 N. A. Barlev, L. Liu, N. H. Chehab, K. Mansfield, K. G. Harris, T. D. Halazonetis and S. L. Berger, *Mol. Cell*, 2001, **8**, 1243–1254.
14 J. S. Akella, D. Wloga, J. Kim, N. G. Starostina, S. Lyons-Abbott, N. S. Morrissette, S. T. Dougan, E. T. Kipreos and J. Gaertig, *Nature*, 2009, **467**, 218–222.
15 M. Orpinell, M. Fournier, A. Riss, Z. Nagy, A. R. Krebs, M. Frontini and L. Tora, *EMBO J.*, 2010, **29**, 2381–2394.
16 J. H. Patel, Y. Du, P. G. Ard, C. Phillips, B. Carella, C. J. Chen, C. Rakowski, C. Chatterjee, P. M. Lieberman, W. S. Lane, G. A. Blobel and S. B. McMahon, *Mol. Cell. Biol.*, 2004, **24**, 10826–10834.
17 J. Vervoorts, J. M. Luscher-Firzlaff, S. Rottmann, R. Lilischkis, G. Walsemann, K. Dohmann, M. Austen and B. Luscher, *EMBO Rep.*, 2003, **4**, 484–490.
18 A. L. Clayton, S. Rose, M. J. Barratt and L. C. Mahadevan, *EMBO J.*, 2000, **19**, 3714–3726.
19 M. E. Terret, R. Sherwood, S. Rahman, J. Qin and P. V. Jallepalli, *Nature*, 2009, **462**, 231–234.
20 S. J. Wort, M. Ito, P. C. Chou, S. K. Mc Master, R. Badiger, E. Jazrawi, P. de Souza, T. W. Evans, J. A. Mitchell, L. Pinhu, K. Ito and I. M. Adcock, *J. Biol. Chem.*, 2009, **284**, 24297–24305.
21 E. J. Lim, T. X. Lu, C. Blanchard and M. E. Rothenberg, *J. Biol. Chem.*, 2011, **286**, 13193–13204.
22 D. N. Lavery and C. L. Bevan, *J. Biomed. Biotechnol.*, 2011, **2011**, 862125.
23 S. Mujtaba, Y. He, L. Zeng, A. Farooq, J. E. Carlson, M. Ott, E. Verdin and M. M. Zhou, *Mol. Cell*, 2002, **9**, 575–586.
24 M. Di Padova, G. Caretti, P. Zhao, E. P. Hoffman and V. Sartorelli, *J. Biol. Chem.*, 2007, **282**, 37650–37659.
25 L. P. van der Heide and M. P. Smidt, *Trends Biochem. Sci.*, 2005, **30**, 81–86.
26 M. A. Martinez-Balbas, U. M. Bauer, S. J. Nielsen, A. Brehm and T. Kouzarides, *EMBO J.*, 2000, **19**, 662–671.
27 C. D. Allis, S. L. Berger, J. Cote, S. Dent, T. Jenuwien, T. Kouzarides, L. Pillus, D. Reinberg, Y. Shi, R. Shiekhattar, A. Shilatifard, J. Workman and Y. Zhang, *Cell*, 2007, **131**, 633–636.
28 F. J. Dekker and H. J. Haisma, *Drug Discovery Today*, 2009, **14**, 942–948.
29 S. D. Furdas, K. Srinivasaraghavan, W. Sippl and M. Jung, *Arch. Pharm. Chem. Life Sci.*, 2012, **345**, 17–21.
30 M. W. Rekowski and A. Giannis, *Biochim. Biophys. Acta, Gen. Subj.*, 2010, **1799**, 760–767.
31 S. D. Furdas, S. Shekfeh, E. M. Bissinger, J. M. Wagner, S. Schlimme, V. Valkov, M. Hendzel, M. Jung and W. Sippl, *Bioorg. Med. Chem.*, 2011, **19**, 3678–3689.
32 E. D. Eliseeva, V. Valkov, M. Jung and M. O. Jung, *Mol. Cancer Ther.*, 2007, **6**, 2391–2398.
33 M. Ghizzoni, A. Boltjes, C. Graaf, H. J. Haisma and F. J. Dekker, *Bioorg. Med. Chem.*, 2010, **18**, 5826–5834.
34 E. M. Bowers, G. Yan, C. Mukherjee, A. Orry, L. Wang, M. A. Holbert, N. T. Crump, C. A. Hazzalin, G. Liszczak, H. Yuan, C. Larocca, S. A. Saldanha, R. Abagyan, Y. Sun, D. J. Meyers, R. Marmorstein, L. C. Mahadevan, R. M. Alani and P. A. Cole, *Chem. Biol.*, 2010, **17**, 471–482.
35 R. Heinke, A. Spannhoff, R. Meier, P. Trojer, I. Bauer, M. Jung and W. Sippl, *ChemMedChem*, 2009, **4**, 69–77.
36 J. Kublbeck, J. Jyrkkarinne, A. Poso, M. Turpeinen, W. Sippl, P. Honkakoski and B. Windshugel, *Biochem. Pharmacol.*, 2008, **76**, 1288–1297.
37 U. Uciechowska, J. Schemies, R. C. Neugebauer, E. M. Huda, M. L. Schmitt, R. Meier, E. Verdin, M. Jung and W. Sippl, *ChemMedChem*, 2008, **3**, 1965–1976.
38 L. M. Szewczuk, S. A. Saldanha, S. Ganguly, E. M. Bowers, M. Javoroncov, B. Karanam, J. C. Culhane, M. A. Holbert, D. C. Klein, R. Abagyan and P. A. Cole, *J. Med. Chem.*, 2007, **50**, 5330–5338.
39 A. Clements, J. R. Rojas, R. C. Trievel, L. Wang, S. L. Berger and R. Marmorstein, *EMBO J.*, 1999, **18**, 3521–3532.
40 C. M. Kim and P. A. Cole, *J. Med. Chem.*, 2001, **44**, 2479–2485.
41 T. M. Bridges, J. E. Marlo, C. M. Niswender, C. K. Jones, S. B. Jadhav, P. R. Gentry, H. C. Plumley, C. D. Weaver, P. J. Conn and C. W. Lindsley, *J. Med. Chem.*, 2009, **52**, 3445–3448.
42 L. T. Bogolyubskaya, V. A. Bogolyubskii and Z. P. Sytnik, *J. Org. Chem. USSR (Engl. Trans.)*, 1966, **2**, 1311–1313.
43 L. G. S. Brooker, R. H. Keyes, R. H. Spragne, R. H. VanDyke, E. Vanlare, G. VanZandt and F. L. White, *J. Am. Chem. Soc.*, 1951, **73**, 5326–5332.
44 R. T. Pardasani, P. Pardasani, A. Jain and S. Kohli, *Phosphorus, Sulfur Silicon Relat. Elem.*, 2003, **179**, 1569–1575.

This journal is © The Royal Society of Chemistry 2012

Med. Chem. Commun., 2012, **3**, 305–311 | 311